

Nephrol Dial Transplant (2008) 23: 82–90  
 doi: 10.1093/ndt/gfm699  
 Advance Access publication 31 October 2007



## Original Article

# Effect of oral calcium carbonate on aortic calcification in apolipoprotein E-deficient (apoE<sup>-/-</sup>) mice with chronic renal failure

Olivier Phan<sup>1,4,\*</sup>, Ognen Ivanovski<sup>1,5,\*</sup>, Igor G. Nikolov<sup>1,3</sup>, Nobuhiko Joki<sup>1</sup>, Julien Maizel<sup>3</sup>, Loïc Louvet<sup>3</sup>, Maud Chasseraud<sup>3</sup>, Thao Nguyen-Khoa<sup>1,2</sup>, Bernard Lacour<sup>2</sup>, Tilman B. Drüeke<sup>1</sup> and Ziad A. Massy<sup>3</sup>

<sup>1</sup>Inserm, Unit 845, Necker Hospital, Université Paris V, Paris, France, <sup>2</sup>Laboratory of Biochemistry A, Necker Hospital, Université Paris V, Paris, France, <sup>3</sup>Inserm, ERI-12, University of Picardie and Amiens University Hospital, Amiens, France, <sup>4</sup>Department of Nephrology, Centre Hospitalier Universitaire Vaudois, Lausanne, Switzerland and <sup>5</sup>Department of Urology, University Clinical Centre, Medical Faculty, Skopje, Republic of Macedonia

### Abstract

**Background.** In chronic kidney disease (CKD) patients, the intake of calcium-based phosphate binders is associated with a marked progression of coronary artery and aortic calcification, in contrast to patients receiving calcium-free phosphate binders. The aim of this study was to reexamine the role of calcium carbonate in vascular calcification and to analyse its effect on aortic calcification-related gene expression in chronic renal failure (CRF).

**Methods.** Mice deficient in apolipoprotein E underwent either sham operation or subtotal nephrectomy to create CRF. They were then randomly assigned to one of the three following groups: a control non-CRF group and a CRF group fed on standard diet, and a CRF group fed on calcium carbonate enriched diet, for a period of 8 weeks. Aortic atherosclerotic plaque and calcification were evaluated using quantitative morphologic image processing. Aortic gene and protein expression was examined using immunohistochemistry and Q-PCR methods.

**Results.** Calcium carbonate supplementation was effective in decreasing serum phosphorus but was associated with a higher serum calcium concentration. Compared with standard diet, calcium carbonate enriched diet unexpectedly induced a significant decrease of both plaque ( $p < 0.05$ ) and non-plaque-associated calcification surface ( $p < 0.05$ ) in CRF mice. It also increased osteopontin (OPN) protein expression in atherosclerotic lesion areas of aortic root. There was also a numerical increase in OPN and osteoprotegerin gene expression in total thoracic aorta but the difference did not reach the level of significance. Finally, calcium carbonate did not change the severity of atherosclerotic lesions.

**Conclusion.** In this experimental model of CRF, calcium carbonate supplementation did not accelerate but instead decreased vascular calcification. If our observation can be extrapolated to humans, it appears to question the contention that calcium carbonate supplementation, at least when given in moderate amounts, necessarily enhances vascular calcification. It is also compatible with the hypothesis of a preponderant role of phosphorus over that of calcium in promoting vascular calcification in CRF.

**Keywords:** atherosclerosis; calcification; calcium carbonate; CKD; phosphate; uraemia

### Introduction

Extensive atherosclerosis and vascular calcification are common complications of advanced chronic kidney disease (CKD). They are associated with each other [1] and with a high incidence of cardiovascular events and mortality. The factors involved in these complications are complex. Numerous metabolic and endocrine abnormalities involving calcium and phosphorus metabolism are found in CKD [2–4]. Furthermore, CKD is believed to be a state of inflammation and oxidative stress [5–7]. Most of these abnormalities occur early in the course of chronic renal failure (CRF) and may contribute to the development and progression of vascular calcification and atherosclerosis [8].

The mechanisms regulating the process of vascular calcification and the factors involved are subject to continued investigation. Both calcium and phosphorus directly stimulate vascular smooth muscle cell transformation into osteoblast-like cells and abnormal mineralization *in vitro* [9–11]. In addition, numerous other factors have been shown, both *in vitro* and *in vivo* [12–15], to promote this process, in part through the production and activity of proteins like osteopontin (OPN), osteoprotegerin (OPG),

Correspondence and offprint requests to: Prof. Ziad A. Massy, MD, PhD, Inserm ERI-12, Divisions of Clinical Pharmacology and Nephrology, University of Picardie and Amiens University Hospital, Av. Rene Laennec, F-80054 Amiens, France. Tel: + 33 3 2245 5788; Fax: + 33 3 2245 5660; E-mail: massy@u-picardie.fr

\*Dr. Olivier Phan and Dr Ognen Ivanovski contributed equally to this work.

osteocalcin, bone morphogenic proteins and matrix Gla protein [16].

In clinical studies in CKD patients, hypercalcaemia and hyperphosphataemia have also been found to be associated with the vascular calcification process [17,18]. The recent recognition of hyperphosphataemia as a predictor of cardiac and all-cause mortality [19,20] points to the necessity of phosphate-lowering treatments. This includes the oral administration of traditional calcium-based phosphate binders and, more recently, of calcium-free compounds such as sevelamer hydrochloride and lanthanum carbonate. In three randomized controlled trials in chronic haemodialysis patients, the administration of calcium-based phosphate binders was associated with marked progression of coronary artery and aortic calcification, in contrast to patients receiving sevelamer treatment [21,22], and with higher mortality [23]. However, in these studies, it was not possible to include non treated groups or histological analyses of vascular calcification such as those which can be done in animal models.

We decided to address the question of the role of calcium-containing phosphate binders in arterial calcification and atherosclerosis in a common model of rapidly progressive atherosclerosis, namely the apolipoprotein E-deficient (apoE<sup>-/-</sup>) mouse. When superimposing CRF in this model, according to a recently established method, severe vascular calcification occurs spontaneously together with accelerated atheroma progression [24,25]. Extensive aortic calcium phosphate deposits are observed both in atheromatous plaque ('intima') and non-plaque areas ('media') [25].

The goal of the present study was to examine in this mouse model the hypothesis of an acceleration of cardiovascular calcification by calcium carbonate, and if so, to evaluate whether calcium deposits were limited to the non-plaque areas, plaque areas, or both. We also tested the effect of CRF and calcium carbonate respectively on aortic gene expression of OPG and OPN, both involved in the regulation of the vascular calcification process [26,27] and also on the aortic protein expression of OPN.

## Methods

### *Animals*

Female, 8-week-old apoE<sup>-/-</sup> homozygous mice were initially obtained from Charles Rivers Breeding Laboratories (Wilmington, MA, USA) and subsequently bred in our animal facility. Since it has been shown that in 16-week-old apoE<sup>-/-</sup> mice, atherosclerotic plaque formation is two to three times greater in female than in male animals [25], we used only female mice. All procedures were in accordance with the National Institutes of Health (NIH) guidelines for care and use of experimental animals (NIH publication No. 85-23). The mice were housed in polycarbonate cages in a pathogen-free, temperature-controlled (25°C) facility, with a strict 12-h light-dark cycle and free access to standard diet and water. The powder diet (Harlan Teklad Global Diet 2018, Harlan, UK) contained 18.9% protein, 6% fat, 1.01% calcium, 0.65% phosphorus, 1.55 calcium/phosphorus ratio and 1.54 IU/g vitamin D3. This is a regular diet which is widely used in animal facilities and whose phosphorus

content is not high. Calcium carbonate was administered as a 3% mix, together with the standard diet to one mouse group for a period of 8 weeks.

### *Experimental procedure and diet*

At the age of 10 weeks, we created CRF in apoE<sup>-/-</sup> mice according to a previously reported two-step procedure [25]. Briefly, at the age of 8 weeks, we applied cortical electrocautery to the right kidney through a 2 cm flank incision, and performed left total nephrectomy through a similar contralateral incision at the age of 10 weeks. Special care was taken to avoid damage to the adrenals. Other mice underwent a two-step procedure of sham surgery with decapsulation of both kidneys and a 14-day distance between the two operations. Blood samples were taken 2 weeks after nephrectomy. Non-CRF mice (20 animals, serum urea, 7–10 mM) were put on standard diet. CRF mice were randomized, based on serum urea levels (>20 mM) to two experimental groups receiving either standard diet plus 3% calcium carbonate (CaCO<sub>3</sub>) supplementation (25 animals) or standard diet alone (25 animals). The mortality noted in both the CRF groups was approximately 20%, mostly due to excessively severe uraemia following the operation. In order to perform Q-PCR analysis of aortic lesion gene expression, we did experiments in a supplementary series of animals undergoing the same experimental procedure as above. We present the biochemical and tissue analyses obtained in these two animal series together.

At the end of the study, mice were sacrificed under anaesthesia with ketamin/xylazine (100 mg/kg, 20 mg/kg) and whole blood was collected via cardiac puncture. Subsequently, the heart and aorta were dissected and freed from connective tissues. Dissected aortas were fixed in 4% formaldehyde for quantification of atherosclerotic lesions. In the supplementary series of animals, a solution of phosphate-buffered saline (PBS) was perfused through the heart and aorta. The aortas were then handled with sterile surgical instruments, quickly dissected and freed down to the renal arteries, plunged into RNA-later reagent and kept for 24 h at 2–8°C. Finally, they were frozen in RNase-free tubes at –80°C and further analysis of gene Q-PCR expression was performed. In both series of animals, in order to quantify calcium phosphate deposits and atherosclerotic lesion extension and to perform immunohistochemistry analyses at the aortic root site, the aortic roots were separated from the aortas. The aortic root with three visible valves was embedded in Optimal Cutting Temperature (OTC) gel under dissecting microscope and stored at –80°C, as reported previously [25].

### *Total RNA extraction from aorta*

Aortas were surgically removed and stored at –80°C prior to extraction using RNA-later reagent (Qiagen) according to the manufacturer's protocol. Aortas were disrupted in TRI reagent (Sigma Aldrich) using a homogenizer. We then proceeded as described by the manufacturer's protocol till the first centrifugation. After the centrifugation, we immediately removed the top supernatant and mixed with 0.7-fold volume of absolute ethanol. The mix was transferred to the microspin column supplied with the

micro Rneasy total RNA isolation kit (Qiagen). Washing of the column, DNase treatment and elution of RNA were performed using the protocol supplied by Qiagen. Samples of total RNA were quantified using the standard OD<sub>260</sub> method. RNA quality was confirmed by the absence of degradation products after denaturing agarose gel electrophoresis and staining with ethidium bromide.

#### *Serum biochemistry*

Blood was sampled via retro-orbital venous sinus puncture at the time of randomization and at 4 weeks of treatment, and subsequently again at 8 weeks of treatment via cardiac puncture, at the time of sacrifice. The collected blood was put into chilled dry tubes, spun in a refrigerated centrifuge for 10min/10000rpm and stored as serum at  $-80^{\circ}\text{C}$ . Serum levels of urea, calcium, phosphorus and total cholesterol were measured using Hitachi 917 auto analyzer (Roche, Meylan, France), as previously described [25]. Parathyroid hormone (iPTH) was measured using two-site ELISA for the quantitative determination of mouse intact parathyroid hormone levels in serum (Immutopics, San Clemente, California, 96 Test Kit, Cat#60–2300).

#### *Quantification of atherosclerotic plaques and aortic gene expression by reverse transcription reaction and Q-PCR*

Evaluation of the atherosclerotic plaque area was made by 'en face' method described previously [24,28]. Briefly, the aortas were carefully freed of connective and adipose tissue under a dissection microscope, opened longitudinally and stained with Oil red O. The quantification was made with Histolab software (Microvision Instruments, Evry, France), as reported [25]. The extent of atherosclerosis was expressed as the percentage of surface area of the aorta covered by lesions. We performed two series of experiments. In the first series, we examined atherosclerotic plaques in the thoracic aorta, while in the second series, the thoracic aortas were used to examine gene expression.

The aortic expression of the selected genes was analysed by Q-PCR with an ABI prism 7900 HT (Applied Biosystems). The eluted RNA was used in a reverse transcription reaction. The cDNA was made from 0.5  $\mu\text{g}$  total RNA from one mouse aorta using high capacity cDNA Archive Kit (Applied Biosystems) in a 20  $\mu\text{l}$  reaction at  $37^{\circ}\text{C}$  for 2 h. Q-PCR was done in a 20  $\mu\text{l}$  volume containing 1  $\mu\text{l}$  of reverse transcription products and 0.5  $\mu\text{mol/l}$  of each primer, diluted 1:2 with SYBR Green I Master Mix (Applied Biosystems). The primers and gene product sizes were 5'-tccaatgctccctacagtcga-3' and 5'-aggtcctcatctgtggcatca-3' (126 bp) for OPN; 5'-aagagcaaaccttccagctgc-3' and 5'-cgctgcttcacagaggtcaa-3' (102 bp) for OPG; and 5'-gggtatggaatcctgtggcat-3' and 5'-ttcagcatcctgtcagcaatg-3' (143 bp) for  $\beta$ -actin. All primers were obtained from Eurogentec. Amplification by Q-PCR was performed as follows: 1 cycle of  $95^{\circ}\text{C}$  for 10 min and 40 cycles of  $95^{\circ}\text{C}$  for 15 s,  $60^{\circ}\text{C}$  for 30 s and  $72^{\circ}\text{C}$  for 30 s, representing the melting, primer annealing and primer extension phases of the reaction, respectively. Following the amplification, a reaction product melt curve was performed to provide evidence for a single reaction product. The correctness was further confirmed after denaturing agarose gel electrophoresis and

staining with ethidium bromide of the Q-PCR products. All mRNA expression data were normalized with the  $\beta$ -actin mRNA expression in the same sample.

#### *Quantitative and qualitative evaluation of aorta calcification*

Vascular calcifications in the aortic root were evaluated by von Kossa staining in 7  $\mu\text{m}$  cryosections of the aortic tissue. Briefly, the cryosections were placed in 5% silver nitrate solution (Sigma Aldrich, St. Louis, MO, USA) for 30 min in darkness. Then they were put in revelatory solution (Kodak) for 5 min and fixed in 5% sodium-thiosulphate solution for another 5 min. Finally, they were stained with 2% eosin. Calcium deposits appeared in black on bright red-coloured surrounding tissue. We developed morphologic image-processing algorithms for computer-assisted automated quantitative measurement of calcification from aortic sections revealed by von Kossa silver nitrate staining. Data were expressed as the relative proportion of the calcified area to the total surface area covering either the inside or the outside of atherosclerotic lesions and as the size of calcification granules on either surface, as described previously [29]. We performed statistical analyses in those aortic root samples where we could obtain three visible valves. In order to reduce the observed differences in absolute vascular calcification values between the two different mouse series, we elected to present these data relative to each other after adjustment as follows. We considered as 1 the percentage of vascular calcification found in the mouse of the non-CRF group, which had the closest value to the mean value of the group. Subsequently, the individual values of each vascular calcification measurement from the two experiments were adjusted by this value.

#### *OPN protein expression in aortic root lesions*

Snap frozen 7  $\mu\text{m}$  sections were analysed by immunohistochemical staining for OPN expression. Briefly, the sections were fixed in acetone for 10 min. Endogenous peroxidase was quenched with 2%  $\text{H}_2\text{O}_2$  in methanol for 10 min, followed by a brief rinse in PBS and incubation in 10% bovine serum albumin (BSA) for 1 h. Polyclonal rabbit anti-mouse OPN antibody (Assay Designs Inc., Ann Arbor, MI, USA) was added in blocking buffer (1% BSA in PBS) in a 1:100 dilution and incubated at  $4^{\circ}\text{C}$  overnight. After rinsing with PBS, biotinylated goat anti-rabbit antibody (Vector Laboratories) was added in blocking buffer in a dilution of 1:300 and incubated for 30 min at room temperature. Peroxidase ABC-reagent and AEC (3-Amino-9-Ethyl-Carbazole) chromogenic substrate were applied following a commercial protocol (Vector Laboratories). The OPN expression was analysed inside the atherosclerotic plaque lesions. The representative image of each slide with visible three aortic valves on a  $\times 25$  magnification was captured on a micro-computer equipped with Sony Camera and Histolab software (Microvision Instruments, Evry, France) and analysed by computerized image analysis program. Semiquantitative assessment of OPN staining was done by quantification of brown field expression inside of the three atherosclerotic valve lesions of the aortic root, as previously described for other proteins [24,30].

*Quantification of nitrotyrosine, monocyte-macrophage (MOMA) infiltration and collagen in aortic root lesions*

Lesion nitrotyrosine expression, a marker for oxidative stress in atheromatous lesions and MOMA infiltration and lesion collagen content were assessed as described previously [24]. Briefly, for nitrotyrosine analysis, the 7  $\mu$ m cryosections were preincubated in peroxidase blocking solution (Dako Cytomation, Trappes, France) before incubation with biotinylated nitrotyrosine monoclonal mouse antibody (Cayman Chemical, SpiBio, Massy, France). The sections were treated with peroxidase-labeled streptavidin (Dako) for 15 min, followed by reaction with diaminobenzidine/hydrogen peroxidase. A representative image of each slide with three aortic valves visible on a  $\times 25$  magnification was captured on a microcomputer equipped with Sony Camera and Histolab software (Microvision Instruments, Envy, France) and analysed by computerized image analysis program. Semiquantitative assessment of nitrotyrosine expression was done by semiautomatic quantification of brown field expression specifically inside of the atherosclerotic valve lesions, as described previously [24,30].

For MOMA infiltration, aortic 7  $\mu$ m cryosections were incubated with 10% normal goat serum at room temperature, and incubated with a primary rat monoclonal antibody against mouse macrophages (clone MOMA-2; BioSource International, Camarillo, CA, USA). The secondary antibody was a biotin-horseradish peroxidase-conjugated goat anti-rat IgG (Vector Laboratories, Biovalley, Marne la Vallée, France). Immunostainings were visualized after incubation with a peroxidase detection system (Vectastain ABC kit, Vector Laboratories) using 3-amino 9-ethyl carbazole (Sigma Aldrich) as substrate. Data were analysed as the relative proportion of infiltrated area to lesion total surface area as described previously [29].

The aortic root collagen content in atheromatous lesions was determined by Sirius red staining [25,31] in all aortic roots where three valves were observed. Images of the best aortic root section with three visible aortic valves were captured and analysed as above. We measured the surface of the atherosclerotic lesions in all three valves, and then, the collagen surface stained as red-coloured fields inside the plaque lesions. Results have been expressed as the relative proportion of collagen area to total surface area of atherosclerotic lesions.

*Statistical analysis*

Data were evaluated by analysis of variance (ANOVA), Mann–Whitney test or chi-square test, as appropriate. Results were expressed as means  $\pm$  SEM. Differences between groups were considered significant for  $p < 0.05$ .

**Results**

*Serum biochemistry*

At the time of sacrifice (10 weeks of CRF and 8 weeks of diet), mean body weight was decreased in the CRF mice supplemented with CaCO<sub>3</sub> diet compared with non-CRF mice on standard diet. There was no difference between non-CRF and CRF mice on standard diet (Table 1). Serum urea, total cholesterol and calcium concentrations were significantly increased in both CRF groups, compared with the non-CRF groups (Table 1). CaCO<sub>3</sub> treatment was effective in decreasing serum phosphorus in CRF mice although it was associated with a higher serum calcium concentration than in non-Ca-supplemented CRF mice (Table 1). There was a numerical reduction of serum Ca  $\times$  P product by the CaCO<sub>3</sub> treatment. However, this decrease was not significant (ANOVA global  $p$  value, 0.063). Serum PTH was numerically lower in CRF mice on CaCO<sub>3</sub> diet than in CRF control mice, and comparable to those in non-CRF mice. Unfortunately, only a small number of serum PTH levels measured in CRF mice on CaCO<sub>3</sub> diet fell within the limits of the PTH kit used. Our efforts to obtain additional PTH data in the supplementary mouse series, including the use of another kit, remained unsuccessful.

*Aorta calcification*

We observed two different types of vascular calcification: (i) a solid type of deposit, with one large compact black deposit inside the plaque (Figure 1A) and (ii) another type of deposit with more diffused, punctuated black deposits dispersed throughout the lesion area (Figure 1B and C). We found no relation of the type of deposits with the presence or absence of CRF or with the type of treatment.

Both, plaque and non-plaque vascular calcification were increased in CRF mice compared with non-CRF littermates

**Table 1.** Effect of CaCO<sub>3</sub> supplemented diet on body weight and serum biochemistry

	Non-CRF standard diet <sup>a</sup>	CRF standard diet <sup>b</sup>	CRF CaCO <sub>3</sub> diet <sup>c</sup>	$p$
Body weight g ( $n$ , 20/20/20)	25.7 $\pm$ 0.9	24.0 $\pm$ 0.4	23.2 $\pm$ 0.4 <sup>a</sup>	<0.05
Urea, mmol/l ( $n$ , 19/17/16)	8.9 $\pm$ 0.3	27.0 $\pm$ 1.2 <sup>a</sup>	25.0 $\pm$ 1.4 <sup>a</sup>	<0.0001
Calcium, mmol/l ( $n$ , 18/18/16)	2.32 $\pm$ 0.03	2.54 $\pm$ 0.05 <sup>a</sup>	2.67 $\pm$ 0.06 <sup>a,b</sup>	<0.0001
Phosphorus, mmol/l ( $n$ , 17/17/16)	2.75 $\pm$ 0.26	2.84 $\pm$ 0.18	2.05 $\pm$ 0.18 <sup>a,b</sup>	<0.05
Ca $\times$ P, mmol <sup>2</sup> /l <sup>2</sup> ( $n$ , 17/17/16)	6.30 $\pm$ 0.58	7.16 $\pm$ 0.49	5.40 $\pm$ 0.45	0.063
PTH, ng/ml* ( $n$ , 9/6/3)	39 $\pm$ 9	124 $\pm$ 29	26 $\pm$ 7	
Total cholesterol, mmol/l ( $n$ , 17/15/15)	11.2 $\pm$ 0.3	15.3 $\pm$ 0.6 <sup>a</sup>	13.9 $\pm$ 0.6 <sup>a</sup>	<0.0001

CRF indicates chronic renal failure. Data were analysed by ANOVA (means  $\pm$  SEM),  $p$  stands for global  $p$  of ANOVA. Treatment groups: non-CRF on standard diet, CRF on standard diet and CRF on CaCO<sub>3</sub> supplemented diet,  $n$  is the number of mice. Superscript letters show significant difference to corresponding group ( $p < 0.05$ ). \*Serum PTH could be measured in limited number of mice.

**Table 2.** Effect of CaCO<sub>3</sub> supplementation on thoracic aorta plaque area and plaque-associated collagen content and OPN expression at aortic root site

	Non-CRF standard diet <sup>a</sup>	CRF standard diet <sup>b</sup>	CRF CaCO <sub>3</sub> diet <sup>c</sup>	<i>p</i>
Thoracic aorta lesion area % ( <i>n</i> , 9/11/11)	0.52 ± 0.06	1.16 ± 0.17 <sup>a</sup>	0.80 ± 0.16	<0.05
Plaque collagen content % ( <i>n</i> , 9/9/9)	42.4 ± 2.2	55.2 ± 2.6 <sup>a</sup>	55.7 ± 2.9 <sup>a</sup>	<0.001
Mice with positive OPN staining % ( <i>n</i> , 6/8/6)	50	12.5	83.3 <sup>b</sup>	<0.03

CRF indicates chronic renal failure. Data were analysed by ANOVA for plaque area and for collagen content (means ± SEM) and by Chi-square test for OPN, *p* stands for global *p*. Treatment groups: non-CRF on standard diet, CRF on standard diet and CRF on CaCO<sub>3</sub> supplemented diet, *n* is the number of mice. Superscript letters show significant difference to corresponding group (*p* < 0.05).

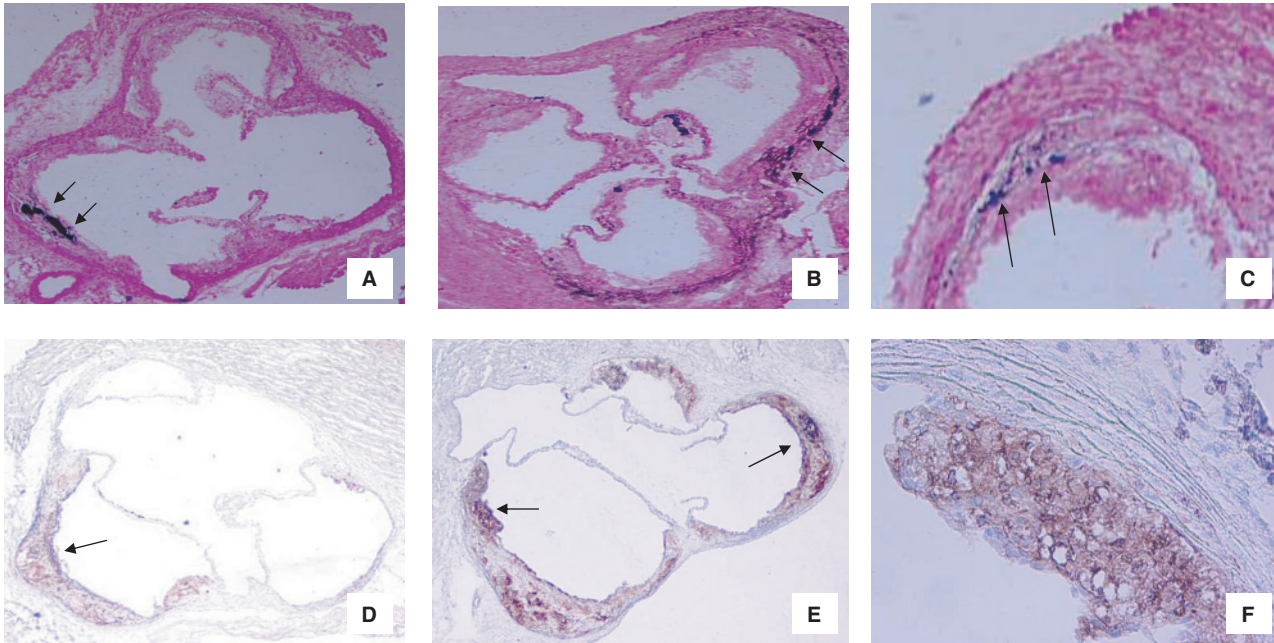


**Fig. 1.** (A–C) Extent and localization of different types of atherosclerotic lesion calcification in apoE<sup>-/-</sup> mice without CRF receiving standard diet or in apoE<sup>-/-</sup> mice with CRF receiving either CaCO<sub>3</sub> supplemented diet or standard control diet. von Kossa staining: (A) solid type of plaque calcification, magnification ×25; (B) non-plaque calcification, magnification ×25; (C) diffuse type of plaque calcification, magnification ×100. (D–F) Immunohistochemical visualization of osteoprotegerin (OPN) protein expression in apoE<sup>-/-</sup> mice without CRF receiving standard diet or in apoE<sup>-/-</sup> mice with CRF receiving either CaCO<sub>3</sub> supplemented diet or standard control diet. (D) CRF mice on standard diet, with three visible aortic valves and low OPN expression (brown) in only one of the valvular lesions, magnification ×25; (E) CRF mice on CaCO<sub>3</sub> diet, with three visible valves and marked OPN expression (dark brown) in all three valvular lesions, magnification ×25; (F) OPN expression in aortic root valve lesion in CRF mice on CaCO<sub>3</sub> diet, magnification ×100.

(Figures 2A, B and C). CaCO<sub>3</sub> supplementation induced a significant decrease in both types of calcification, compared with no CaCO<sub>3</sub> supplementation (Figures 2A, B and C).

#### Aortic atheromatous lesions and gene expression

In the CRF mice, atherosclerotic lesions on the longitudinal aorta were increased, compared with non-CRF littermates. The administration of a CaCO<sub>3</sub> diet did not significantly change the extent of atherosclerotic lesions in CRF mice (Table 2).

For the assessment of possible differences of aortic gene expression between non-CRF and CRF mice on normal diet or on CaCO<sub>3</sub> supplemented diet (Figure 3), we analyzed aortic tissues from the aortic root down to the abdominal part of the aorta using Q-PCR. There was a significant increase of OPG gene expression in both CRF mouse groups, compared with the non-CRF mice. The numerical

increase in CRF mice in response to CaCO<sub>3</sub> supplementation, compared with CRF mice on standard diet, however, did not reach the level of statistical significance (Figure 3). As to OPN, there was no difference in its gene expression between non-CRF and CRF mice on standard diet. Although CaCO<sub>3</sub> supplementation of CRF mice enhanced its expression by two-fold compared with CRF mice on standard diet, this difference was not significant. The difference of OPN expression between CRF CaCO<sub>3</sub> mice and control mice on standard diet also was not significant.

#### OPN protein expression in atherosclerotic lesions of the aortic root

By immunostaining, OPN expression in aortic root lesions was increased in CRF mice on CaCO<sub>3</sub> diet, compared to CRF mice (Figure 1D) on standard diet (Table 2 and Figure 1E and F). There was no difference between the two CRF and non-CRF control groups.

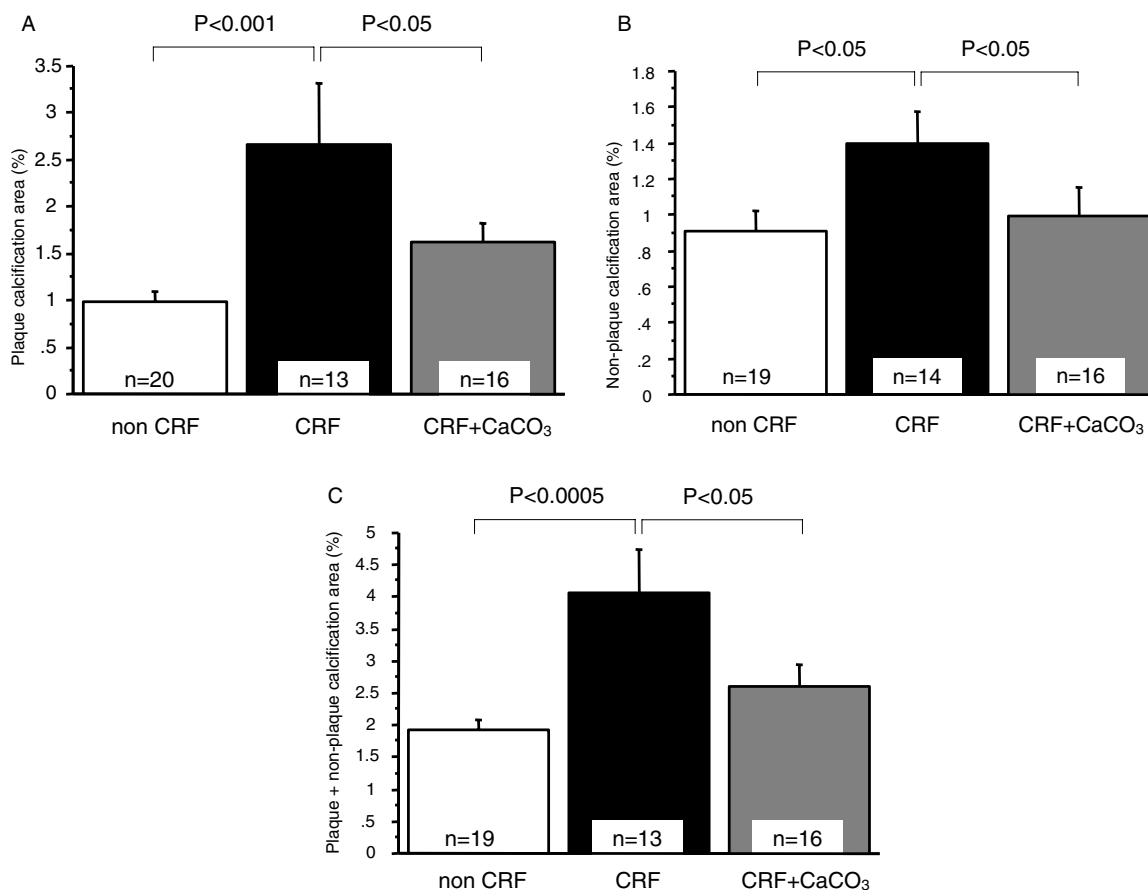


**Fig. 2.** (A) Plaque calcifications in apoE<sup>-/-</sup> mice without CRF receiving standard diet or in apoE<sup>-/-</sup> mice with CRF receiving either CaCO<sub>3</sub> supplemented diet or standard control diet. Values at the time of sacrifice reflecting the proportion of calcified plaque area to the total surface area of atherosclerotic lesions in apoE<sup>-/-</sup> mice. Analysis by ANOVA. (B) Non-plaque calcifications in apoE<sup>-/-</sup> mice without CRF receiving standard diet or in apoE<sup>-/-</sup> mice with CRF receiving either CaCO<sub>3</sub> supplemented diet or standard diet. Values at the time of sacrifice reflecting the proportion of calcified non-plaque area to the total surface area outside of atherosclerotic lesions in apoE<sup>-/-</sup> mice. Analysis by ANOVA. (C) Plaque and non-plaque aortic calcifications in apoE<sup>-/-</sup> mice without CRF receiving standard diet or in apoE<sup>-/-</sup> mice with CRF receiving either CaCO<sub>3</sub> supplemented diet or standard diet. Values at the time of sacrifice reflecting the proportion of plaque and non-plaque associated calcified area together versus total surface area. Analysis by ANOVA.

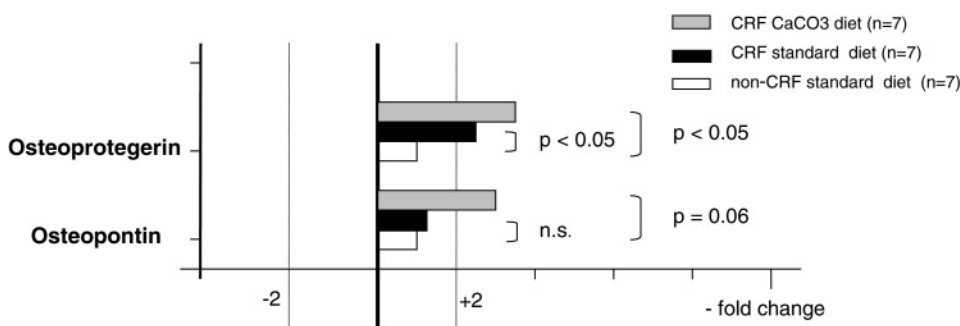


**Fig. 3.** Patterns of aortic gene expression of OPN and OPG in apoE<sup>-/-</sup> mice without CRF receiving standard diet or in apoE<sup>-/-</sup> mice with CRF receiving either CaCO<sub>3</sub> supplemented diet or standard diet. Aortic gene expression was determined with Q-PCR. *n* is the number of aortas analysed in each group. Analysis by Mann-Whitney test.

*Nitrotyrosine expression, MOMA infiltration and collagen content in aortic lesions*

CaCO<sub>3</sub> diet did not lead to a reduction in nitrotyrosine expression in atheromatous plaques, as compared to non-

CRF and CRF control mice (data not shown). The percentage of cross-sectional lesion area occupied by macrophages, as revealed by MOMA-2 staining, was also comparable for the three non-CRF and CRF mice groups (data not shown). Finally, collagen content was significantly increased in both

CRF mouse groups compared to non-CRF mice. CaCO<sub>3</sub> supplementation did not induce a change of collagen content (Table 2).

## Discussion

In the present study, we unexpectedly found an inhibitory effect of CaCO<sub>3</sub> on the lesion severity in both plaque ('intima') and non-plaque ('media') calcification in our experimental model of CRF apoE<sup>-/-</sup> mice. This inhibitory effect occurred despite an increase in serum calcium concentration. Serum phosphorus concentration decreased significantly although the Ca × P product remained unchanged. The inhibitory effect was associated with a two-fold increase of OPN gene expression in total aorta (not statistically significant) and a significant increase in OPN protein expression in aortic lesion areas, compared with control CRF mice. We did not find evidence of changes in local markers of inflammation (MOMA-2 staining) or oxidative stress (nitrotyrosine expression) in response to the CaCO<sub>3</sub> treatment. Finally, the degree of aorta atherosclerosis did not differ between Ca-supplemented and control CRF mice.

The present results are not in accord with the general assumption that the high intestinal calcium absorption subsequent to the ingestion of large amounts of calcium-containing phosphate binders necessarily promotes vascular calcification, even in the absence of hypercalcaemia [22,32]. They, therefore, appear to be at variance with several retrospective clinical studies which showed a correlation between cumulative oral calcium load and vascular calcification among CKD patients receiving CaCO<sub>3</sub> or calcium acetate treatment [17,33]. Of note, the association of calcium-based phosphate binders with active vitamin D derivatives for the treatment of secondary hyperparathyroidism may further enhance intestinal calcium absorption, and in addition that of phosphate, and cause an oversuppression of parathyroid gland function [34].

In the CRF apoE<sup>-/-</sup> mice of the present study, CaCO<sub>3</sub> induced a decrease of serum phosphorus concentration in CRF mice on CaCO<sub>3</sub> diet compared with non-calcium-supplemented mice, although serum calcium and Ca × P product were increased. Unfortunately, we were unable to measure serum 1,25-diOH-vitamin D due to insufficient availability of blood at the time of sacrifice. It is of note that our CRF model is characterized by a constant increase in serum Ca and a variable increase in serum PTH, often in the absence of an elevation of serum phosphorus, together with a striking acceleration of atherosclerosis and vascular calcification, compared with non-CRF mice [25,30]. Interestingly, recent studies clearly demonstrated a major, active role of phosphate in blood vessel calcification, both *in vitro* [9,10,35] and *in vivo* [36,37]. Of particular importance, is the observation by Murshed *et al* [38], who showed in a gene knock-out animal model that two genes were necessary, but also sufficient to trigger ectopic calcification, namely TNAP, an enzyme that cleaves pyrophosphate into two phosphate ions, and type I collagen.

In the present study, we were able to observe an inhibitory effect of CaCO<sub>3</sub> on vascular calcification at two different

sites of the aorta, namely within atheromatous lesions and outside the lesions. Since serum calcium, which was elevated in CRF mice without calcium supplementation, increased to even higher levels in calcium-supplemented CRF mice, the beneficial effect of CaCO<sub>3</sub> on vascular calcification could be explained, at least partially, by the improved control of hyperphosphataemia.

An alternative explanation for the observed decrease in vascular calcification by CaCO<sub>3</sub> diet in this model could be through an effect on calcification regulatory factors expressed by vascular smooth muscle cells after their transformation into osteoblast-like cells. These factors either inhibit or promote the calcification process. OPN is one of them. It is generally considered as an inhibitor of calcification [9]. In the present study, we observed an increase of plaque OPN protein expression at the aortic root site in CRF mice on CaCO<sub>3</sub> diet compared with CRF controls. We also observed an up to two-fold increase of both OPN and OPG gene expression in total thoracic aorta. However, this increase was not significant, maybe due to the relatively small number of aortas available for this analysis. Upregulation of OPN and OPG expression could be interpreted as protective mechanisms against the observed increase in vascular calcification in CRF mice. In line with this observation, Moe *et al.* recently demonstrated an increased expression of OPN in the medial layer of arteries from chronic dialysis patients. Positive staining for OPN and other bone matrix molecules was strongly correlated with medial calcification [38]. Moreover, OPN was expressed in the intima of calcified arteries of such patients [39]. Finally, the addition of uraemic serum also increased OPN expression in bovine vascular smooth muscle cells *in vitro* [40]. Recently, it was shown in another mouse model that calcification of the vascular tissue was preceded by local induction of OPN expression [41]. We have to point out that any failure to observe significant changes in aortic protein and gene expression could be due to either real absence of changes or technical reasons, including the semiquantitative nature of immunohistochemistry methods used for the study of proteins. Another problem that we faced was that of the PTH measurements. The widely used so-called 'mouse' Intact PTH ELISA was actually developed for studies in rats. Results obtained with this method in normal versus CRF mice proved to be extremely heterogeneous.

CaCO<sub>3</sub> did not reduce aortic plaque area, in contrast to our previous demonstration of a decrease in the degree of both calcification and atherosclerosis in response to the phosphate binder sevelamer [30] and the calcimimetic R-568 [42], respectively. One of the observed differences between these studies is an increase in serum calcium in response to CaCO<sub>3</sub>, as compared to no change in serum calcium in response to sevelamer and a decrease in response to R-568. Whether the difference in the degree of hypercalcaemia plays any role in the development of atherosclerosis remains to be seen.

Since hyperphosphataemia also appears to play an important role in vascular calcification, it is of interest to note that a graded independent relation has been found between increasing levels of serum phosphate and the relative risk of cardiovascular events and death both in patients with CKD [19,43] and in patients without CKD [44].

The control of hyperphosphataemia by CaCO<sub>3</sub> probably is better than the absence of such control, at least in terms of vascular calcification, as shown in the present study and the study by Cozzolino *et al.* [45]. These authors also observed a decrease in aorta calcification in response to CaCO<sub>3</sub> administration. However, CaCO<sub>3</sub> is probably less potent than the calcium-free phosphate binder sevelamer in retarding vascular disease progression and improving survival, as suggested by a recent controlled study in incident haemodialysis patients comparing calcium-containing phosphate binders with sevelamer [23].

In conclusion, CaCO<sub>3</sub> given for the control of hyperphosphataemia in CRF does not necessarily enhance the progression of arterial calcification, compared with uncontrolled hyperphosphataemia. Based on our present observation in a CRF mouse model, it may even exert a protective effect, at least in presence of an increased Ca × P product. Our finding is compatible with a more important role of phosphorus than of calcium in promoting vascular calcification in the setting of CRF.

**Acknowledgements.** O.P. was funded by a grant from SICPA foundation, Lausanne, Switzerland. O.I. and I.G.N. were recipients of a grant from EGIDE Foundation, Paris, France. N.J. was supported by Toho University funds, Japan. A part of this work has been presented in abstract form and as a poster at the 2004 annual convention of the American Society of Nephrology in Saint Louis, MO, USA and at the 2006 43rd ERA-EDTA Congress in Glasgow, UK.

**Conflict of interest statement.** None declared.

(See related article by Markus Ketteler and Patrick Biggar. After several years of witchhunting, can calcium-based phosphate binding be released on probation? *Nephrol Dial Transplant* 2008; 23: 17–19.)

## References

- Haydar AA, Hujairi NM, Covic AA *et al.* Coronary artery calcification is related to coronary atherosclerosis in chronic renal disease patients: a study comparing EBCT-generated coronary artery calcium scores and coronary angiography. *Nephrol Dial Transplant* 2004; 19: 2307–2312
- Block G, Port FK. Calcium phosphate metabolism and cardiovascular disease in patients with chronic kidney disease. *Semin Dial* 2003; 16: 140–147
- Nishizawa Y, Shoji T, Emoto M *et al.* Roles of metabolic and endocrinological alterations in atherosclerosis and cardiovascular disease in renal failure: another form of metabolic syndrome. *Semin Nephrol* 2004; 24: 423–425
- Rostand SG, Drueke TB. Parathyroid hormone, vitamin D, and cardiovascular disease in chronic renal failure. *Kidney Int* 1999; 56: 383–392
- Himmelfarb J, Stenvinkel P, Ikizler TA *et al.* The elephant in uremia: oxidant stress as a unifying concept of cardiovascular disease in uremia. *Kidney Int* 2002; 62: 1524–1538
- Massy ZA, Maziere C, Kamel S *et al.* Impact of inflammation and oxidative stress on vascular calcifications in chronic kidney disease. *Pediatr Nephrol* 2005; 20: 380–382
- Nguyen-Khoa T, Massy ZA, De Bandt JP *et al.* Oxidative stress and haemodialysis: role of inflammation and duration of dialysis treatment. *Nephrol Dial Transplant* 2001; 16: 335–340
- Mitsnefes MM, Kimball TR, Kartal J *et al.* Cardiac and vascular adaptation in pediatric patients with chronic kidney disease: role of calcium-phosphorus metabolism. *J Am Soc Nephrol* 2005; 16: 2796–2803
- Giachelli CM, Speer MY, Li X *et al.* Regulation of vascular calcification: roles of phosphate and osteopontin. *Circ Res* 2005; 96: 717–722
- Jono S, McKee MD, Murry CE *et al.* Phosphate regulation of vascular smooth muscle cell calcification. *Circ Res* 2000; 87: E10–E17
- Reynolds JL, Joannides AJ, Skepper JN *et al.* Human vascular smooth muscle cells undergo vesicle-mediated calcification in response to changes in extracellular calcium and phosphate concentrations: a potential mechanism for accelerated vascular calcification in ESRD. *J Am Soc Nephrol* 2004; 15: 2857–2867
- Bostrom K, Watson KE, Horn S *et al.* Bone morphogenetic protein expression in human atherosclerotic lesions. *J Clin Invest* 1993; 91: 1800–1809
- Luo G, Ducy P, McKee MD *et al.* Spontaneous calcification of arteries and cartilage in mice lacking matrix GLA protein. *Nature* 1997; 386: 78–81
- Schafer C, Heiss A, Schwarz A *et al.* The serum protein alpha 2-Heremans-Schmid glycoprotein/fetuin-A is a systemically acting inhibitor of ectopic calcification. *J Clin Invest* 2003; 112: 357–366
- Shanahan CM, Cary NR, Salisbury JR *et al.* Medial localization of mineralization-regulating proteins in association with Monckeberg's sclerosis: evidence for smooth muscle cell-mediated vascular calcification. *Circulation* 1999; 100: 2168–2176
- Moe SM, Chen NX. Pathophysiology of vascular calcification in chronic kidney disease. *Circ Res* 2004; 95: 560–567
- Goodman WG, Goldin J, Kuizon BD *et al.* Coronary-artery calcification in young adults with end-stage renal disease who are undergoing dialysis. *N Engl J Med* 2000; 342: 1478–1483
- Moe SM. Vascular calcification and renal osteodystrophy relationship in chronic kidney disease. *Eur J Clin Invest* 2006; 36: 51–62
- Block GA, Hulbert-Shearon TE, Levin NW *et al.* Association of serum phosphorus and calcium x phosphate product with mortality risk in chronic hemodialysis patients: a national study. *Am J Kidney Dis* 1998; 31: 607–617
- Block GA, Klassen PS, Lazarus JM *et al.* Mineral metabolism, mortality, and morbidity in maintenance hemodialysis. *J Am Soc Nephrol* 2004; 15: 2208–2218
- Block GA, Spiegel DM, Ehrlich J *et al.* Effects of sevelamer and calcium on coronary artery calcification in patients new to hemodialysis. *Kidney Int* 2005; 68: 1815–1824
- Chertow GM, Burke SK, Raggi P. Sevelamer attenuates the progression of coronary and aortic calcification in hemodialysis patients. *Kidney Int* 2002; 62: 245–252
- Block GA, Raggi P, Bellasi A *et al.* Mortality effect of coronary calcification and phosphate binder choice in incident hemodialysis patients. *Kidney Int* 2007; 71: 438–441
- Ivanovski O, Szumilak D, Nguyen-Khoa T *et al.* The antioxidant N-acetylcysteine prevents accelerated atherosclerosis in uremic apolipoprotein E knockout mice. *Kidney Int* 2005; 67: 2288–2294
- Massy ZA, Ivanovski O, Nguyen-Khoa T *et al.* Uremia accelerates both atherosclerosis and arterial calcification in apolipoprotein E knockout mice. *J Am Soc Nephrol* 2005; 16: 109–116
- Speer MY, McKee MD, Guldberg RE *et al.* Inactivation of the osteopontin gene enhances vascular calcification of matrix Gla protein-deficient mice: evidence for osteopontin as an inducible inhibitor of vascular calcification in vivo. *J Exp Med* 2002; 196: 1047–1055
- Min H, Morony S, Sarosi I *et al.* Osteoprotegerin reverses osteoporosis by inhibiting endosteal osteoclasts and prevents vascular calcification by blocking a process resembling osteoclastogenesis. *J Exp Med* 2000; 192: 463–474
- Ivanovski O, Szumilak D, Nguyen-Khoa T *et al.* Dietary salt restriction accelerates atherosclerosis in apolipoprotein E-deficient mice. *Atherosclerosis* 2005; 180: 271–276
- Angulo JN-KT, Massy Z, Drueke T, Serra J. Morphological quantification of aortic calcification from low magnification images. *Image Anal Stereol* 2003; 22: 81–89
- Phan O, Ivanovski O, Nguyen-Khoa T *et al.* Sevelamer prevents uremia-enhanced atherosclerosis progression in apolipoprotein E-deficient mice. *Circulation* 2005; 112: 2875–2882
- Mallat Z, Gojova A, Marchiol-Fournigault C *et al.* Inhibition of transforming growth factor-beta signaling accelerates atherosclerosis and induces an unstable plaque phenotype in mice. *Circ Res* 2001; 89: 930–934



32. Burke SK, Dillon MA, Hemken DE *et al.* Meta-analysis of the effect of sevelamer on phosphorus, calcium, PTH, and serum lipids in dialysis patients. *Adv Ren Replace Ther* 2003; 10: 133–145
33. Guerin AP, London GM, Marchais SJ *et al.* Arterial stiffening and vascular calcifications in end-stage renal disease. *Nephrol Dial Transplant* 2000; 15: 1014–1021
34. Goodman WG. Medical management of secondary hyperparathyroidism in chronic renal failure. *Nephrol Dial Transplant* 2003; 18: iii2–iii8
35. Jakoby MG IV, Semenkovich CF. The role of osteoprogenitors in vascular calcification. *Curr Opin Nephrol Hypertens* 2000; 9: 11–15
36. Murshed M, Harmey D, Millan JL *et al.* Unique coexpression in osteoblasts of broadly expressed genes accounts for the spatial restriction of ECM mineralization to bone. *Genes Dev* 2005; 19: 1093–1104
37. Stubbs JR, Liu S, Tang W *et al.* Role of hyperphosphatemia and 1,25-dihydroxyvitamin d in vascular calcification and mortality in fibroblastic growth factor 23 null mice. *J Am Soc Nephrol* 2007; 18: 2116–2124
38. Moe SM, O'Neill KD, Duan D *et al.* Medial artery calcification in ESRD patients is associated with deposition of bone matrix proteins. *Kidney Int* 2002; 61: 638–647
39. Moe SM, Duan D, Doehle BP *et al.* Uremia induces the osteoblast differentiation factor Cbfa1 in human blood vessels. *Kidney Int* 2003; 63: 1003–1011
40. Chen NX, O'Neill KD, Duan D *et al.* Phosphorus and uremic serum up-regulate osteopontin expression in vascular smooth muscle cells. *Kidney Int* 2002; 62: 1724–1731
41. Westenfeld R, Schafer C, Smeets R *et al.* Fetuin-A (AHSG) prevents extraosseous calcification induced by uraemia and phosphate challenge in mice. *Nephrol Dial Transplant* 2007; 22: 1537–1546
42. Ivanovski O, Phan O, Nikolov GI *et al.* The calcimimetic R-568 prevents progression of calcification and atherosclerosis in apolipoprotein E deficient (EKO) mice with chronic renal failure (CRF) and secondary hyperparathyroidism (HPT). *J Am Soc Nephrol* 2006; 17: 690A
43. Kimata N, Akiba T, Pisoni RL *et al.* Mineral metabolism and haemoglobin concentration among haemodialysis patients in the Dialysis Outcomes and Practice Patterns Study (DOPPS). *Nephrol Dial Transplant* 2005; 20: 927–935
44. Tonelli M, Sacks F, Pfeffer M *et al.* Relation between serum phosphate level and cardiovascular event rate in people with coronary disease. *Circulation* 2005; 112: 2627–2633
45. Cozzolino M, Staniforth ME, Liapis H *et al.* Sevelamer hydrochloride attenuates kidney and cardiovascular calcifications in long-term experimental uremia. *Kidney Int* 2003; 64: 1653–1661

*Received for publication: 12.7.06*

*Accepted in revised form: 10.9.07*